BIOCHEMISTRY
including biophysical chemistry & molecular biology

Article

pubs.acs.org/biochemistry

Hysteresis and Negative Cooperativity in Human UDP-Glucose Dehydrogenase

Renuka Kadirvelraj,[†] Nicholas C. Sennett,[†] Gregory S. Custer,[†] Robert S. Phillips,[†,‡] and Zachary A. Wood*[,†]

[†]Department of Biochemistry and Molecular Biology and [‡]Department of Chemistry, University of Georgia, Athens, Georgia 30602, United States

ABSTRACT: Human UDP-α-D-glucose 6-dehydrogenase (hUGDH) forms a hexamer that catalyzes the NAD^+-dependent oxidation of UDP-α-D-glucose (UDG) to produce UDP-α-D-glucuronic acid. Mammalian UGDH displays hysteresis (observed as a lag in progress curves), indicating that the enzyme undergoes a slow transition from an inactive to an active state. Here we show that hUGDH is sensitive to product inhibition during the lag. The inhibition results in a systematic decrease in steady-state velocity and makes the lag appear to have a second-order dependence on enzyme concentration. Using transient-state kinetics, we confirm that the lag is in fact due to a substrate and cofactor-induced isomerization of the enzyme. We also show that the cofactor binds to the hUGDH:UDG complex with negative cooperativity. This suggests that the isomerization may be related to the formation of an asymmetric enzyme complex. We propose that the hysteresis in hUGDH is the consequence of a functional adaptation; by slowing the response of hUGDH to sudden increases in the flux of UDG, the other biochemical pathways that use this important metabolite (i.e., glycolysis) will have a competitive edge.

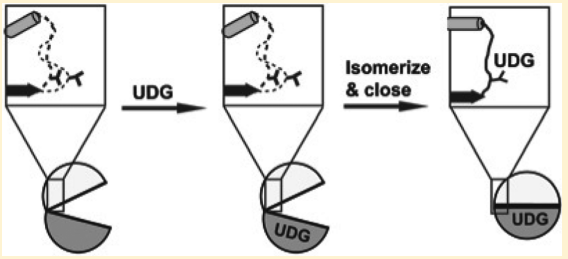

UDP-α-D-glucose 6-dehydrogenase (UGDH) catalyzes the NAD^+-dependent oxidation of UDP-α-D-glucose (UDG) to produce UDP-α-D-glucuronic acid (UGA) (Figure 1A).[1−3] Dickinson first identified bovine UGDH as a hysteretic enzyme on the basis of his observation of a lag in enzyme progress curves before steady-state velocity was attained.[4] Hysteresis occurs when an enzyme undergoes a slow transition from a less active to a more active state.[5,6] This transient phase can be an important step in the regulation of enzyme activity. For example, hysteresis in pancreatic glucokinase plays an essential role in insulin signaling; the slow response of the enzyme means that a brief spike in serum glucose levels will not stimulate the release of insulin.[7−9]

The transient phase in hysteretic enzymes is typically associated with one of three distinct models: (i) the dissociation of an inactive aggregate, (ii) an enzyme polymerizing to form an active complex, and (iii) a slow isomerization to a more active conformation.[5,10−14] Dickinson reported that the specific activity of bovine UGDH decreases at high enzyme concentrations and, in support of the first model, suggested the concentration-dependent dissociation of an inactive aggregate to an active form.[4] In contrast, we have shown that human UGDH (hUGDH) dimers undergo a concentration-dependent association to form a discrete, active hexamer (Figure 1B).[15,16] Cofactor binding can also induce the formation of this hexamer.[16] Thus, our results suggest that the lag may be due to the association of dimers to form a higher-activity hexamer.

The crystal structures of hUGDH reveal a doughnut-shaped hexamer of point group symmetry 32 that is formed by the oligomerization of three dimers (Figure 1B).[15,17] During the catalytic cycle, the UDG and NAD^+ binding domains of adjacent dimers rotate in a concerted manner to allow substrate binding and product release (Figure 1C).[16] These domain rotations resemble a clamshell motion and can occur without disrupting the hexamer.[15] The dynamic nature of the hUGDH hexamer suggests that enzyme isomerization may also play a role in enzyme hysteresis. However, neither the association nor the isomerization models of hUGDH can explain Dickinson's report of lower specific activity at high enzyme concentrations.[4]

The goal of this study is to identify the underlying mechanism for hysteresis in hUGDH. Here we report a detailed analysis of the steady-state and transient-state kinetics of the enzyme at physiological pH. We show that the lag is actually due to a substrate and cofactor-induced isomerization of the hUGDH hexamer to form an active, asymmetric complex. The possible physiological relevance of the hysteresis in hUGDH is discussed.

MATERIALS AND METHODS

Enzyme Assays. The nucleotides NAD^+, NADH, and UDG were obtained from Sigma. The expression and purification of the recombinant wild-type enzyme and the $hUGDH_{K94E}$ construct have been described in detail elsewhere.[15,18] All experiments were conducted in a reaction buffer containing 50 mM Hepes (pH 7.5), 50 mM NaCl, and 5 mM

Received: November 27, 2012
Revised: January 29, 2013
Published: January 30, 2013

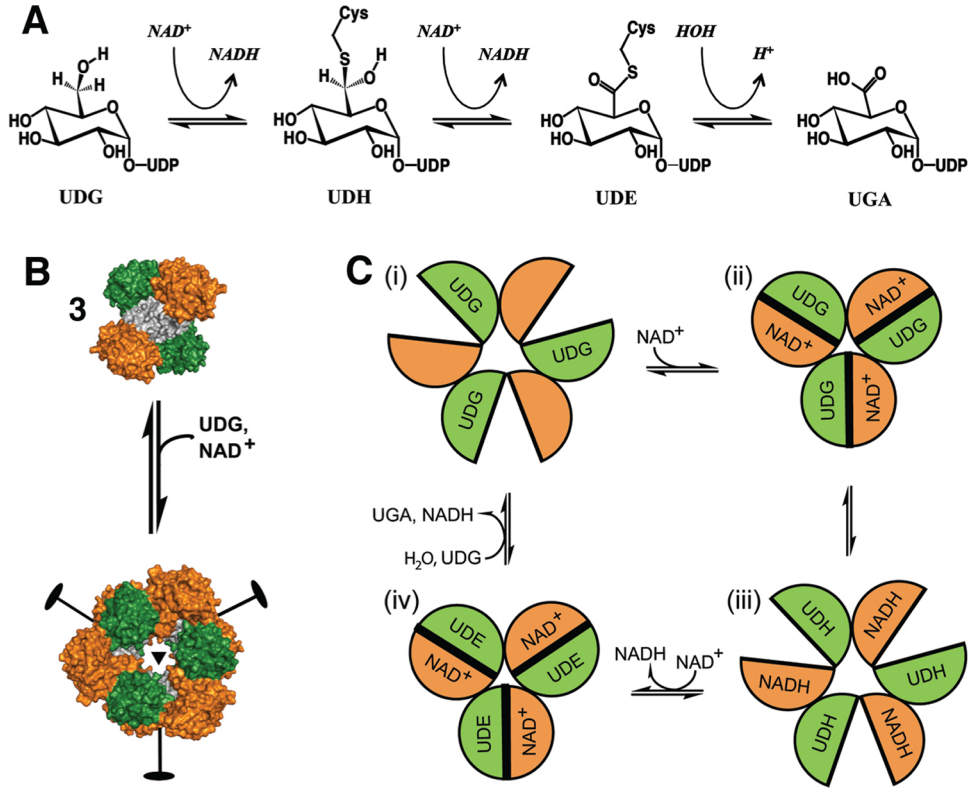

Figure 1. Catalytic cycle of hUGDH. (A) UGDH uses two molecules of NAD^+ to catalyze the oxidation of UDP-α-D-glucose (UDG) to UDP-α-D-glucuronic acid (UGA). First, NAD^+ oxidizes UDG to an aldehyde, which reacts with Cys276 to form a thiohemiacetal intermediate (UDH). A second NAD^+ molecule oxidizes UDH to a thioester intermediate (UDE). Finally, UDE is hydrolyzed to form the product, UDP-glucuronic acid (UGA). (B) Three hUGDH dimers undergo a concentration-dependent association to form the active hexamer. The formation of the hexamer can also be induced by substrate and cofactor binding.[16] hUGDH nucleotide-sugar (green) and cofactor binding (orange) and dimerization (grey) domains are depicted, and the 32 symmetry of the hexamer is indicated. (C) Domain rotation facilitates substrate binding and product release during the hUGDH catalytic cycle, without dissociating the hexamer.[15] The cartoon depicts the nucleotide-sugar (orange) and cofactor binding (green) domains for the top trimer of hUGDH. (i) Catalysis begins with UDG binding to the open domain conformation. (ii) The binding of the cofactor results in domain closure. (iii) NAD^+ oxidizes UDG to UDH, and the domains rotate open. (iv) NADH is exchanged for a second molecule of NAD^+, and the domains close. Finally, UDH is oxidized to UDE, which is then hydrolyzed to produce UGA.

EDTA. Unless otherwise stated, 230 nM enzyme was used in all assays. For steady-state analysis, the enzymes and substrates were preincubated separately for 5 min at 25 °C and the reaction was initiated by a rapid manual mixing of the two solutions. An Agilent 8453 UV−vis spectrometer equipped with a Peltier temperature controller was used to follow enzyme reactions by continually monitoring the formation of NADH at 340 nm (molar absorptivity coefficient of 6220 M^{-1} cm^{-1}). Steady-state kinetic analysis of wild-type hUGDH was conducted using saturating amounts of 2.5 mM NAD^+ and 0.3 mM UDG. Because of the lower activity, steady-state analysis of $hUGDH_{K94E}$ required an enzyme concentration of 9.1 μM. For $hUGDH_{K94E}$, higher concentrations of substrates were needed to reach saturation (30 mM NAD^+ and 10 mM UDG). Steady-state velocities were measured after the lag period. All data were analyzed and modeled using nonlinear regression as implemented in PRISM (GraphPad Software Inc., San Diego, CA). The substrate saturation curves were fit to either a hyperbolic or a sigmoidal model based on residual analysis:[19,20]

$$v_0 = \frac{k_{cat}[E_t][S]^h}{K_m{}^h + [S]^h} \quad (1)$$

To determine the K_i for the competitive inhibitor NADH, steady-state analysis was conducted using the conditions described above in the presence of two different concentrations of NADH, 30 and 70 μM. We used the apparent K_m from each concentration of NADH to calculate a K_i using eq 2 and averaged the results:

$$K_m^{app} = K_m\left(1 + \frac{[I]}{K_i}\right) \quad (2)$$

Cofactor Binding Assays. hUGDH fluorescence binding titrations were performed at 25 °C using reaction volumes of 2 mL. Solutions of hUGDH (with or without 0.3 mM UDG) and NADH (concentration ranging from 2 to 200 μM) were preincubated separately for 5 min at 25 °C and then quickly mixed to initiate binding. The volume of NADH added was less than 3% of the total reaction volume. All measurements were recorded at 1 s intervals using a Perkin-Elmer LS55 luminescence spectrometer with excitation and emission wavelengths of 285 and 335 nm, respectively, and both slit widths set to 8.8 nm. The raw data were systematically corrected for the inner filter effect[21,22] using the molar absorptivity of NADH at the tryptophan excitation and emission wavelengths (ε_{285} = 2101 M^{-1} cm^{-1} and ε_{335} = 6132 M^{-1} cm^{-1}, respectively). Binding of NADH to hUGDH

dx.doi.org/10.1021/bi301593c | Biochemistry 2013, 52, 1456−1465

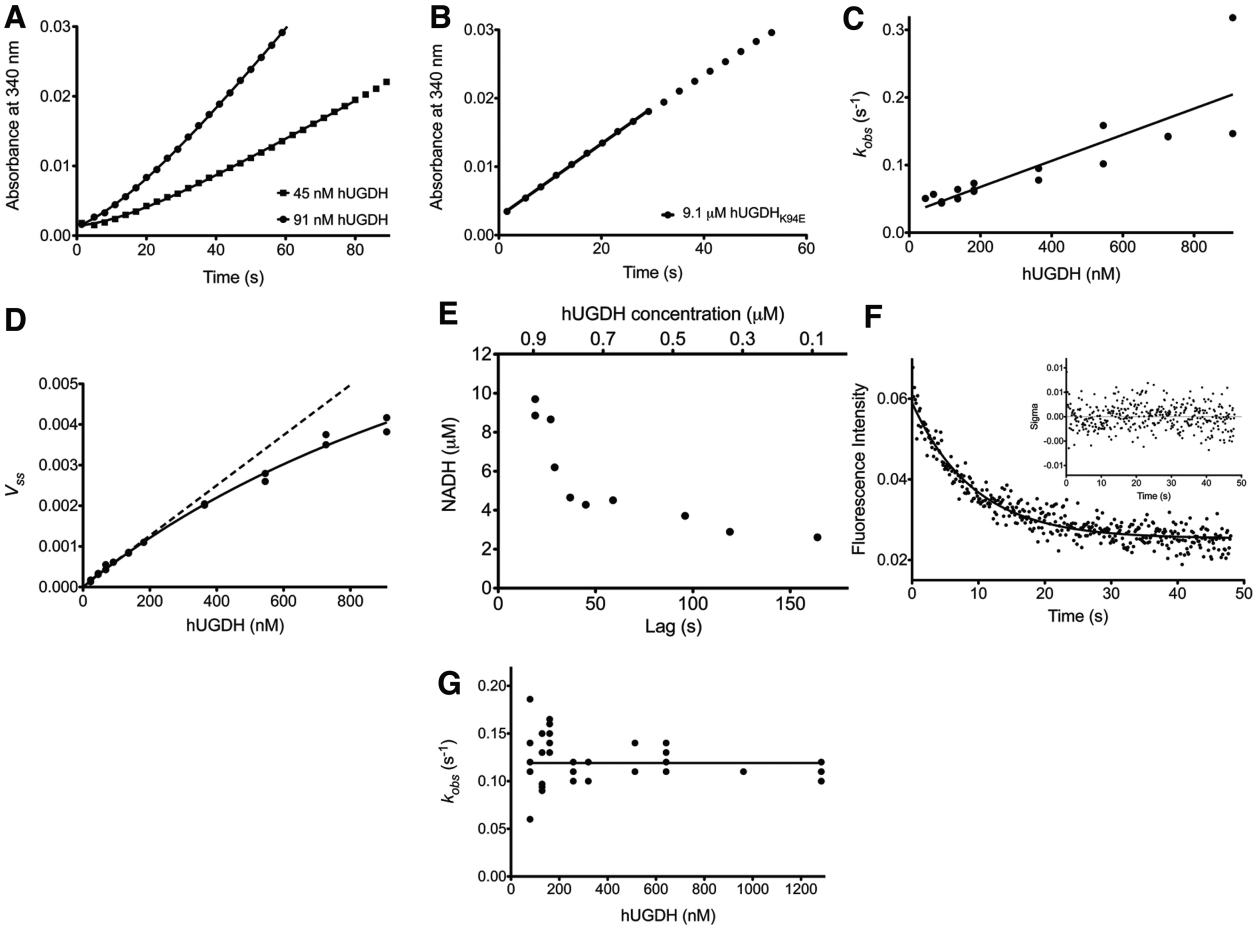

Figure 2. The lag in hUGDH progress curves is due to enzyme isomerization. (A) Progress curves of 45 (■) and 91 nM hUGDH (●) show a lag in the rate of product formation. Data are modeled (—) using eq 4 (see the text). (B) Progress curves of 9.1 μM hUGDH$_{K94E}$ dimer do not show a lag. The solid line depicts the linear area used to calculate the steady-state velocity. (C) The dependence of the relaxation rate constant (k_{obs}) on hUGDH concentration. (D) hUGDH steady-state velocity shows a systematic decrease with increasing enzyme concentration that is consistent with product inhibition (—). The expected linear steady-state velocity in the absence of these effects is shown as a dotted line. (E) The lag for each hUGDH concentration was plotted versus the amount of NADH produced during that time frame. Lower values of the lag correspond to higher enzyme concentrations. The plot shows that at higher hUGDH concentrations, inhibitory levels of NADH [K_i = 27 ± 3 μM (see Table 1)] accumulate by the time the enzyme reaches the steady-state. (F) Representative stopped-flow kinetic data showing hysteresis for the formation of the abortive hUGDH:UDG:NADH ternary complex. The binding of UDG and NADH to 513 nM hUGDH quenches the intrinsic tryptophan fluorescence (●). The process is modeled as a single-exponential decay (—). The inset shows the residual plot for the fit. (G) The relaxation rate constant for formation of the hUGDH:UDG:NADH complex (k_{obs}) shows a first-order dependence on enzyme concentration, indicating a slow isomerization.

quenches the intrinsic protein fluorescence of the enzyme and was analyzed by plotting the ΔF ($F_o - F_f$) versus NADH concentration (see Results). The dissociation constant (K_d) and Hill coefficient (h) were calculated by fitting the data to either a hyperbolic or a sigmoidal model based on residual analysis:[19,20]

$$\Delta F = \frac{\Delta F_{max}[L]^h}{K_d{}^h + [L]^h} \quad (3)$$

Transient-State Kinetics. Stopped-flow studies were conducted at 25 °C using an Applied Photophysics SX18-MV spectrophotometer with a dead time of ~1.2 ms. Preincubation with saturating concentrations of UDG (0.3 mM) or NADH (0.35 mM) was used to form the appropriate binary complexes. The change in the intrinsic tryptophan fluorescence of hUGDH or preformed complexes upon rapid mechanical mixing with UDG or NADH was continuously monitored over time. An excitation wavelength of 285 nm and an emission filter with a cutoff below 320 nm were used for data collection. Scans were collected for short periods of 0.2, 0.5, or 1 s to follow the fast processes. Longer periods of data collection (1−200 s) were used to record the slow events. The data were fit to the appropriate equations for decay to obtain the change in fluorescence (ΔF) (see Results). All spectral data analysis was performed using numerical integration methods with Pro-K from Applied Photophysics.

RESULTS

hUGDH Hysteresis is Due to Enzyme Isomerization. The lag in hUGDH progress curves at physiological pH (7.4) indicates that the enzyme undergoes a slow transformation from a less active to a more active state (Figure 2A). We examined the effect of the oligomeric structure on hysteresis using the K94E substitution in hUGDH (hUGDH$_{K94E}$), which we have previously shown to prevent hexamer formation.[16] Progress curves of hUGDH$_{K94E}$ show no lag, suggesting that

dx.doi.org/10.1021/bi301593c | Biochemistry 2013, 52, 1456−1465

Table 1. hUGDH Steady-State and Equilibrium Binding Studies

enzyme	ligand	K_m (μM)	Hill coefficient (h)	k_{cat} (s^{-1})	K_i (μM)	K_d (μM)
$hUGDH_{K94E}$	UDG	269 ± 16[a]		0.012[a]		
	NAD^+	2919 ± 198		0.055		
hUGDH	UDG	16 ± 0.5[a]		1.4[a]		
	NAD^+	942 ± 142	0.74 ± 0.03[a]	1.8		
	NADH				27 ± 3[b]	31 ± 3[c]
hUGDH:UDG	NADH		0.42 ± 0.05[c]			4 ± 2[c]

[a]The kinetic parameters, K_m, h, and k_{cat}, were calculated using eq 1. [b]The NADH K_i was calculated using eq 2. [c]Parameters from steady-state (K_d) and equilibrium binding studies (K_d and h) were calculated using eq 3.

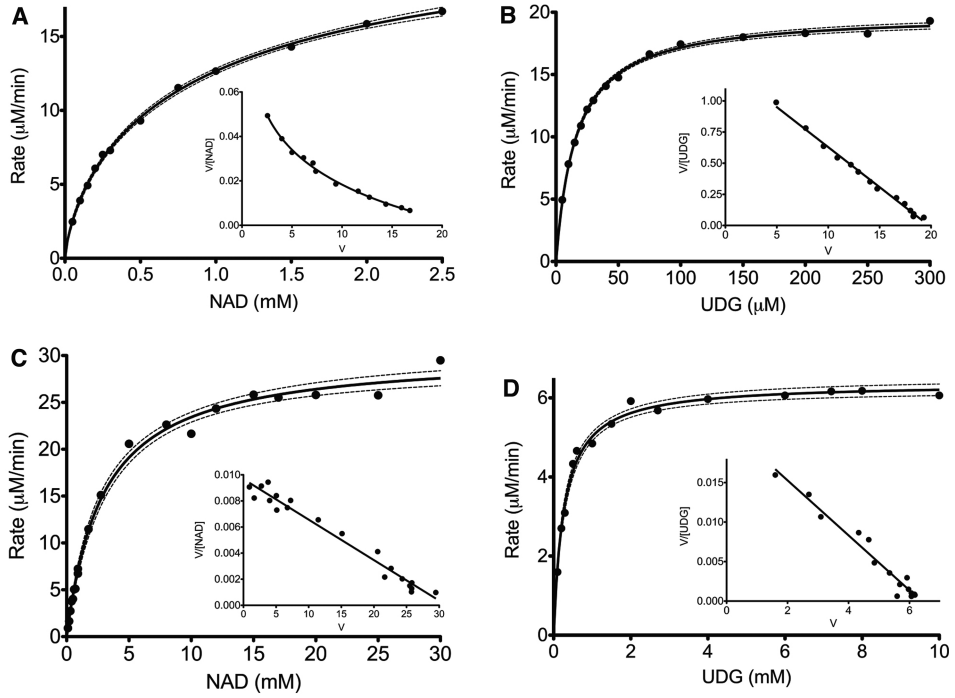

Figure 3. Hexameric hUGDH displays negative cooperativity. (A) hUGDH substrate saturation curves display negative cooperativity with respect to NAD^+. Data were fit to eq 1. The dashed lines indicate the 95% confidence intervals. The inset shows the data linearized in the form of Eadie–Scatchard plots (v/[S] vs v) to illustrate the deviation from hyperbolic kinetics. A concave-up curve denotes negative cooperativity.[37] (B) UDG saturation curves show a hyperbolic dependence (C and D). $hUGDH_{K94E}$ dimer substrate saturation curves display a hyperbolic dependence on NAD^+ and UDG concentration, respectively.

hUGDH hysteresis is due to either formation or isomerization of the hexamer (Figure 2B). We next investigated the effect of enzyme concentration on the lag. Hysteresis can be modeled using the following equation based on relaxation kinetics:[5]

$$P(t) = v_{ss}t - \frac{1}{k_{obs}}(v_{ss} - v_i)(1 - e^{-k_{obs}t}) \quad (4)$$

where P is the concentration of product at time t and k_{obs} is the apparent rate constant for the transition between the initial (v_i) and final steady-state velocities (v_{ss}) (Figure 2A).

This analysis shows that k_{obs} displays a linear dependence on enzyme concentration (Figure 2C). In relaxation kinetics, k_{obs} is proportional to a_0^{n-1}, where a_0 is the total concentration of the reactants that combine to produce the product and n is the order of the reaction.[23] Thus, the non-zero slope of the dependence of k_{obs} on enzyme concentration appears to indicate a second-order reaction and is not consistent with three dimers associating to form a hexamer (a third-order reaction). However, a first-order reaction (enzyme isomerization) could appear to be second-order if significant substrate depletion or product inhibition occurs during the lag.[24,26] Substrate depletion or product inhibition during the lag will occur faster at higher enzyme concentrations. The resulting systematic decrease in steady-state velocity during a first-order isomerization will give the false appearance of a second-order dependence on enzyme concentration (see Discussion). In fact, we do observe a systematic decrease in hUGDH steady-state velocity with increasing enzyme concentration (Figure 2D). This is consistent with Dickinson's earlier report that UGDH specific activity decreases at high enzyme concentrations.[4] At the highest hUGDH concentrations in our assays, only 0.7% and 3.3% of the respective NAD^+ and UDG substrates were consumed during the lag, ruling out substrate depletion as a reason for the decrease in steady-state velocity. On the other hand, mammalian UGDH is known to be sensitive to NADH inhibition, with a reported K_i ranging from 6 to 25 μM.[2,27,28] We have determined the K_i for NADH inhibition under our assay conditions to be 27 ± 3 μM (see Table 1 and a later section). To see if product inhibition could contribute to the systematic decrease in steady-state velocity, we calculated the amount of NADH produced during the lag for different enzyme concentrations (Figure 2E). This analysis shows that significant

dx.doi.org/10.1021/bi301593c | Biochemistry 2013, 52, 1456–1465

levels of NADH accumulate during the lag at higher enzyme concentrations (Figure 2E). Thus, the decrease in steady-state velocity is most likely due to product inhibition.

To avoid product inhibition, we used stopped-flow methods to analyze the formation of the abortive hUGDH:UDG:NADH complex. The binding of substrate and cofactor quenches the intrinsic tryptophan fluorescence of hUGDH (Figure 2F). The decay is best modeled as a single-exponential process:

$$f(t) = Ae^{-k_{obs}t} + \xi(t) + F_f \quad (5)$$

where the fluorescence signal $f(t)$ is related to the amplitude of the process (A), the observed relaxation rate constant (k_{obs}), a noise component [$\xi(t)$], and the plateau of the signal (F_f). k_{obs} shows a first-order dependence on enzyme concentration in the presence of saturating substrate, consistent with hUGDH undergoing a slow isomerization from a less active (E_H) to a more active (E_H*) hexameric state (Figure 2G):

$$E_H{:}UDG{:}NADH \underset{k_r}{\overset{k_f}{\leftrightarrow}} E_H{*}{:}UDG{:}NADH$$

Under saturating substrate conditions, the k_{obs} for the E_H to E_H* isomerization is related to the microscopic rate constants by[23]

$$k_{obs} = k_f + k_r \quad (6)$$

hUGDH Displays Negative Cooperativity during Turnover. We analyzed the steady-state kinetics of hUGDH using an enzyme concentration of 230 nM to reduce the effects of product inhibition (Figure 2D). The substrate saturation curves with respect to NAD^+ display negative cooperativity, with a Hill coefficient (h) of 0.74 ± 0.03 (Figure 3A and Table 1). In contrast, the substrate saturation curves show a hyperbolic dependence on UDG (Figure 3B and Table 1). We next examined the steady-state kinetics of the $hUGDH_{K94E}$ dimer. The substrate saturation curves for NAD^+ and UDG are both hyperbolic, suggesting that the negative cooperativity requires the hexameric complex (Figure 3C,D). Consistent with our previous work,[16] the $hUGDH_{K94E}$ K_m values for NAD^+ and UDG have increased by factors of ~3 and ~17, respectively, indicating that the hexameric complex is important for substrate binding (Table 1). Likewise, the k_{cat} for the dimer has decreased by a factor of ~48, suggesting that the hexamer is important for turnover.

The Abortive Ternary Complex Displays Negative Cooperativity. To rule out a kinetic mechanism for the observed negative cooperativity, we studied the formation of the binary (hUGDH:NADH) and abortive ternary (hUGDH:UDG:NADH) complexes using equilibrium binding experiments. The hysteresis observed in progress curves is also apparent in the binding studies; NADH binding slowly quenches the intrinsic fluorescence of the enzyme in a reaction best modeled as a double-exponential decay (Figure 4A):

$$f(t) = A_{fast}\exp(-k_{fast}t) + A_{slow}\exp(-k_{slow}t) + \xi(t) + F_f \quad (7)$$

where the change in the fluorescence signal, $f(t)$, is related to the amplitudes of the fast and slow processes (A_{fast} and A_{slow}, respectively), the observed rate constants associated with the two events (k_{fast} and k_{slow}, respectively), a noise component [$\xi(t)$], and the plateau of the signal (F_f) for calculating ΔF. The binding of NADH to hUGDH alone is hyperbolic with a K_d of 31 ± 3 μM (Figure 4B and Table 1). In contrast, the binding of NADH to the hUGDH:UDG complex reveals a strong negative cooperativity with a Hill coefficient of 0.42 ± 0.05 (Figure 4C and Table 1). We also observe that the affinity of hUGDH for NADH is increased by ~8-fold in the presence of UDG [K_d = 4 ± 2 μM (Table 1)]. This is consistent with our previous work showing that NADH and UDG interact cooperatively to stabilize the hexamer.[16]

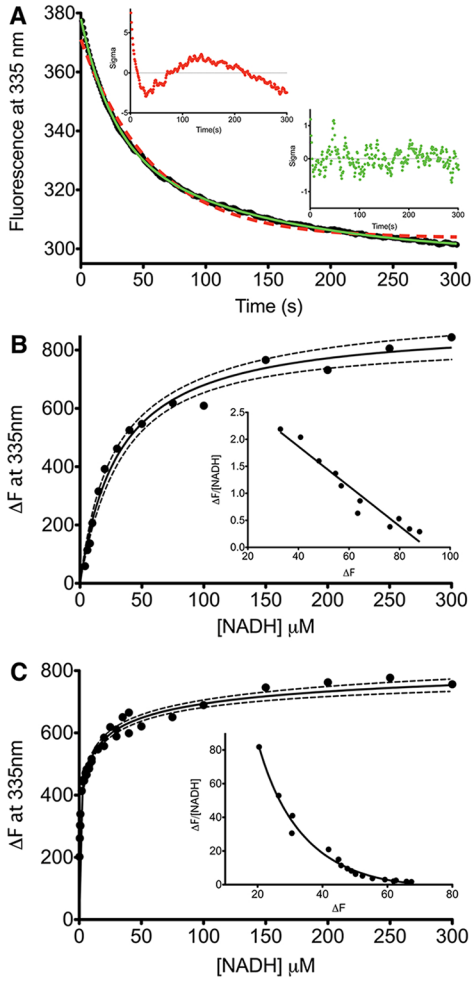

Figure 4. Binding of NADH to the hUGDH:UDG complex reveals hysteresis and strong negative cooperativity. (A) NADH binding slowly quenches the intrinsic tryptophan fluorescence of hUGDH (●). The plot shows a representative example of the fluorescence decay induced by the addition of 40 μM NADH to the enzyme. The process is modeled as both single-exponential (red dashes) and double-exponential (green line) decays. The insets show residual plots for the single-exponential (red) and double-exponential (green) fits, indicating a better fit for the latter. (B) The binding of NADH to hUGDH shows a hyperbolic dependence on NADH concentration. Data were fit to eq 3. The dashed lines indicate the 95% confidence intervals, and the inset depicts an Eadie–Scatchard analysis of the data.[37] (C) The binding of NADH to the hUGDH:UDG complex displays strong negative cooperativity (h = 0.42 ± 0.05).

Transient-State Kinetics Reveals Ligand-Induced Isomerizations in the Formation of the Abortive Ternary Complex. We used stopped-flow to analyze each step in the formation of the abortive ternary complex (hUGDH:UDG:NADH). Each of the following subheadings addresses a specific step in the pathway, and the results are summarized in Figure 7A.

Binding of UDG to hUGDH. Binding of UDG to hUGDH gives a weak change in fluorescence. To improve the signal-to-

dx.doi.org/10.1021/bi301593c | Biochemistry 2013, 52, 1456–1465

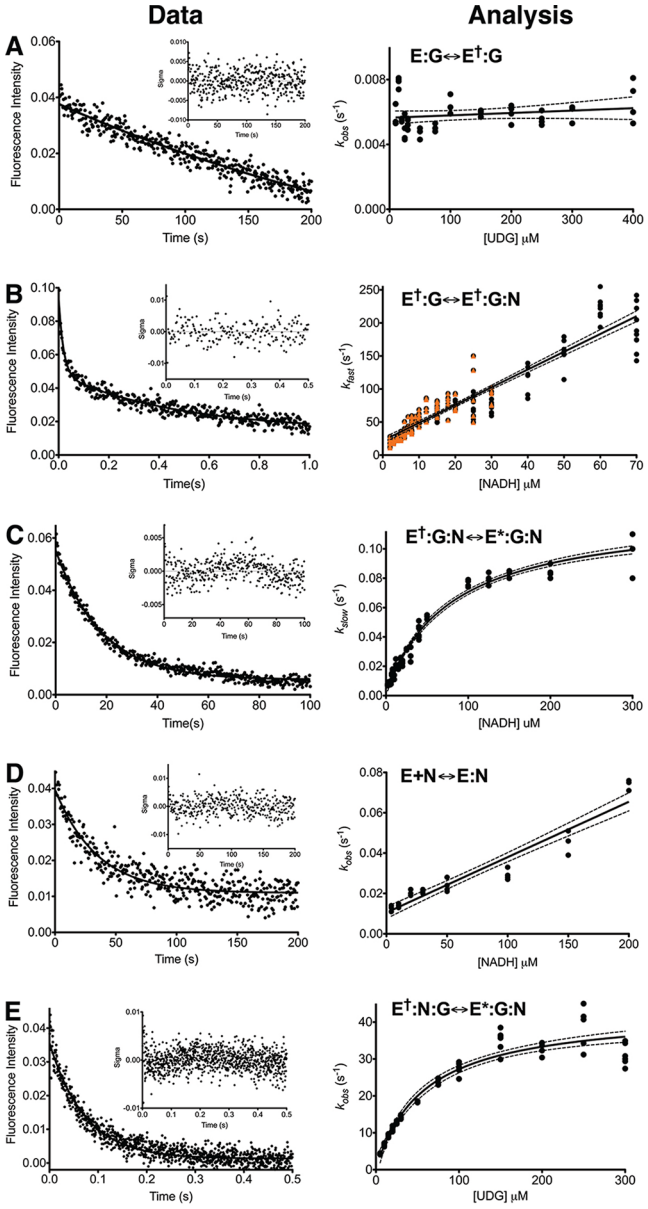

Figure 5. Transient-state kinetics for the stepwise formation of the abortive ternary complex, hUGDH:UDG:NADH. The left column (Data) shows quenching of the intrinsic tryptophan fluorescence (dots) of hUGDH or a preformed hUGDH:ligand complex when it is mixed with UDG or NADH. The process is modeled as a single- or double-exponential decay (—), based on residual analysis (inset). The right column (Analysis) shows the plot of k_{obs} (dots) vs ligand concentration. The solid line represents a linear or hyperbolic model for the event. The dashed lines indicate the 95% confidence intervals. (A) The slow process following the rapid binding of UDG to 430 nM hUGDH is modeled as a single-exponential decay. k_{slow} shows a linear dependence on UDG concentration, albeit with a small, positive slope. The dagger (†) indicates the enzyme has undergone an isomerization. (B) The addition of NADH to the hUGDH†:UDG complex is modeled as a double-exponential decay representing a fast phase (k_{fast}) and a slow phase (k_{slow}). The k_{fast} values determined with 230 nM (orange triangles) and 920 nM (black circles) hUGDH:UDG complex are fit to the same line. (C) Increasing the time intervals allows the slow event following addition of NADH to the hUGDH†:UDG complex to be modeled as a single-exponential decay. The k_{slow} has a hyperbolic dependence on NADH concentration, indicating enzyme isomerization (asterisk). (D) The addition of NADH to hUGDH reveals a slow event, which is modeled as a single-exponential decay. The k_{obs} has a linear dependence on cofactor concentration, consistent with ligand binding. (E) The addition of UDG to the hUGDH:NADH complex is modeled as a single-exponential decay. The k_{obs} for the process displays a hyperbolic dependence on NADH concentration, consistent with an enzyme isomerization (*).

noise ratio, we increased the protein concentration to 460 nM. The decay in fluorescence due to UDG binding reveals two distinct events. The first event terminates in <100 ms and is accompanied by a very small change in fluorescence (ΔF) that falls close to the noise level of the instrument (data not shown). The speed and weak signal prevent us from accurately modeling the process. However, the second, slower event is modeled as a single-exponential decay (Figure 5A). The plot of k_{slow} versus UDG concentration is linear with a small, positive slope (Figure 5A). We interpret the two events to be a fast binding of UDG (G) to the enzyme followed by a relatively slower isomerization of the E:G binary complex to E†:G:

$$E + G \underset{k_{-1}}{\overset{\text{fast } k_1}{\rightleftharpoons}} E{:}G \underset{k_{-2}}{\overset{\text{slow } k_2}{\rightleftharpoons}} E^{\dagger}{:}G$$

A ligand-induced isomerization of an enzyme can be identified by the hyperbolic dependence of the observed rate constant (k_{obs}) on ligand concentration.[23] It is likely that we are only observing the plateau of the hyperbola in Figure 5A. We were unable to sample regions of the hyperbola below 5 μM UDG while maintaining a 10-fold excess of ligand to enzyme concentration. Reducing the enzyme concentration resulted in smaller, noisy amplitudes that complicated our ability to accurately model both processes. As a result, we were not able to determine the microscopic rate constants for the UDG-induced isomerization.

Binding of NADH to the hUGDH†:UDG Complex. The addition of NADH to the hUGDH:UDG complex is best modeled as a double-exponential decay representing a fast phase (k_{fast}) and a slow phase (k_{slow}) (Figure 5B). We were able to measure k_{fast} with 230 nM hUGDH†:UDG complex, but the signal became weak above 30 μM NADH. To increase the signal, we raised the protein concentration to 920 nM to assay higher NADH concentrations. The k_{fast} values from both protein concentrations are fit to the same line; however, fitting the low- and high-protein concentration data separately gives consistent slopes (Figure 5B). The linear dependence of k_{fast} on NADH (N) concentration is consistent with substrate binding:[23]

$$k_{obs} = k_3[N] + k_{-3} \quad (8)$$

Increasing the time interval allows us to accurately model the slow phase as a single-exponential decay (Figure 5C). The k_{slow} reveals a hyperbolic dependence on cofactor concentration and can be modeled with eq 9 (Figure 5C):[23]

$$k_{obs} = \frac{k_4[N]}{K_{eq} + [N]} + k_{-4}, \text{ where } K_{eq} = K_3 = \frac{k_{-3}}{k_3} \quad (9)$$

The forward and reverse rate constants for the fast and slow processes are listed in Table 2 (Figure 7A). Together, the two events are consistent with a two-step equilibrium involving binding and a subsequent ligand-induced enzyme isomerization:

dx.doi.org/10.1021/bi301593c | Biochemistry 2013, 52, 1456−1465

Table 2. Microscopic Rate Constants from hUGDH Transient-State Kinetics

transient event	$k_{forward}$ (k_f, s^{-1})	$k_{reverse}$ (k_r, s^{-1})	k_r/k_f	K_{eq}
$E^{\dagger}$:UDG + NADH ↔ $E^{\dagger}$:UDG:NADH	2.7 ± 0.1 M^{-1} (k_3)[a]	21.9 ± 2 (k_{-3})[a]	8.1	–
$E^{\dagger}$:UDG:NADH ↔ E*:UDG:NADH	(0.12 ± 3) × 10^{-3} (k_4)[b]	(2 ± 1) × 10^{-3} (k_{-4})[b]	0.017	79.3 (K_3)[b]
E + NADH ↔ E:NADH	2.7 × 10^{-4} ± 1.5 × 10^{-5} M^{-1} (k_5)[a]	105 × 10^{-4} ± 1.5 × 10^{-3} (k_{-5})[a]	39	–
$E^{\dagger}$:UDG:NADH ↔ E*:UDG:NADH	42.7 ± 1.4 (k_7)[b]	0.26 ± 1.3 (k_{-7})[b]	0.006	58.3 (K_6)[b]

[a]Forward and reverse rate constants were calculated using eq 8. [b]Forward and reverse rate constants and the equilibrium constant (K_{eq}) were calculated using eq 9.

$$E^{\dagger}{:}G + N \underset{k_{-3}}{\overset{\text{fast } k_3}{\rightleftharpoons}} E^{\dagger}{:}G{:}N \underset{k_{-4}}{\overset{\text{slow } k_4}{\rightleftharpoons}} E^{*}{:}G{:}N$$

However, there is a significant disagreement between the equilibrium constant for the isomerization (K_3 = 79.3) and the dissociation constant for the bimolecular reaction derived from the ratio of the microscopic rate constants (k_{-3}/k_3 = 8.1) (eq 9 and Table 2). This discrepancy may indicate that at least one additional transient process is not detected in the fluorescence decay data (see Discussion).

Binding of NADH to hUGDH. Binding of NADH to hUGDH is modeled as a single-exponential decay. The plot of k_{obs} shows a linear dependence on NADH concentration (Figure 5D). The linearity identifies the event as a second-order process, consistent with a slow binding of the cofactor:

$$E + N \underset{k_{-5}}{\overset{\text{slow } k_5}{\rightleftharpoons}} E{:}N$$

The forward and reverse rate constants for NADH binding were calculated using eq 8 and are listed in Table 2.

Binding of UDG to the hUGDH:NADH Complex. This reaction is modeled as a single-exponential decay (Figure 5E). Plotting k_{obs} reveals a hyperbolic dependence on UDG concentration, indicating a ligand-induced isomerization (Figure 5E):

$$E{:}N + G \underset{k_{-6}}{\overset{\text{fast } k_6}{\rightleftharpoons}} E{:}G{:}N \underset{k_{-7}}{\overset{\text{slow } k_7}{\rightleftharpoons}} E^{*}{:}G{:}N$$

The fact that we do not observe a separate process associated with binding of UDG to the hUGDH:NADH complex suggests that the initial binding event is too fast or the associated amplitudes are too small for us to resolve. Still, the isomerization step is well-modeled using eq 6. The forward and reverse rate constants and the dissociation constant for UDG binding are reported in Table 2.

NADH Inhibition Disrupts Negative Cooperativity in hUGDH. It has been shown that NADH is a competitive inhibitor of mammalian UGDH, with a K_i between 6 and 25 μM.[2,27,28] Here we analyzed product inhibition with NADH under conditions that matched the assays described above. The inhibition assays used 230 nM hUGDH to reduce the effect of endogenous product inhibition due to NADH accumulation during the lag (Figure 2D,E). NADH inhibition shows no significant change in V_{max} but increases the apparent K_m for NAD^+, consistent with competitive inhibition (Figure 6A and Table 1). Using eq 2, an average K_i of 27 ± 3 μM was calculated, in close agreement with previous results. Interestingly, these studies have identified an unusual feature of product inhibition in hUGDH; NADH inhibition abolishes the negative cooperativity observed in steady-state analysis (Figure 6B).

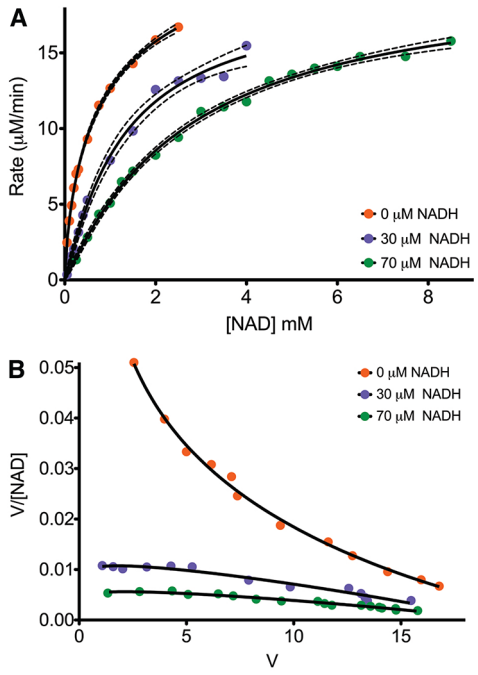

Figure 6. NADH inhibition disrupts hUGDH negative cooperativity. (A) hUGDH substrate saturation plots in the presence of increasing concentrations of NADH [0 (orange), 30 (violet), and 70 μM (green)] show a negligible change in V_{max} but an increase in K_m for NAD^+, indicating competitive inhibition. Data were fit to eq 1. The dashed lines indicate the 95% confidence intervals. (B) The loss of negative cooperativity in the presence of NADH is illustrated by replotting the data from panel A as an Eadie–Scatchard plot.[37] The color scheme is the same as that in panel A.

DISCUSSION

hUGDH Hysteresis is Due to Hexamer Isomerization. We have previously shown that three hUGDH dimers undergo a concentration-dependent association to form the active hexamer.[15,16] We have also shown that hexamer formation can be induced by cofactor binding.[16] Based on these observations, it was reasonable for us to assume the hysteresis in hUGDH might be due to the slow association of the dimers. Because the hexamer is unlikely to dissociate in the highly crowded environment of a cell, hysteresis in hUGDH might simply be the consequence of analyzing the enzyme under dilute conditions. However, our initial analysis of the transient phase of the hUGDH progress curves shows that the dependence of the relaxation rate on enzyme concentration appears to correspond to a second-order process and is not consistent with the association of three dimers to form the active hexamer (a third-order reaction) (Figure 2C).[23] A more detailed analysis reveals a systematic decrease in steady-state velocity at higher enzyme concentrations because of product inhibition (Figure 2D). In fact, we show that inhibitory

dx.doi.org/10.1021/bi301593c | Biochemistry 2013, 52, 1456–1465

concentrations of NADH are produced during the lag (Figure 2E). It is known that hysteresis due to enzyme isomerization (a first-order reaction) can appear to be second-order if product inhibition occurs to a significant extent during the lag phase.[24−26] Briefly, product inhibition will occur faster at higher protein concentrations and cause a systematic decrease in the apparent steady-state velocity. Because the end point of the lag is determined when the enzyme reaches the steady-state, the lag will appear to decrease with an increasing enzyme concentration, resulting in a false second-order dependency. Thus, product inhibition is most likely concealing a first-order isomerization.

To avoid product inhibition, we used stopped-flow methods to study the formation of the abortive ternary complex (hUGDH:UDG:NADH). We show that formation of the hUGDH:UDG:NADH complex also displays hysteresis (Figure 2F). The dependence of the hysteretic relaxation rate on enzyme concentration is first-order, consistent with a slow enzyme isomerization (Figure 2G). Because the rate of isomerization is on the same time scale as the lag in the progress curves, we are analyzing the same process. The progress curves of the $hUGDH_{K94E}$ dimer do not display a lag, suggesting that the isomerization is a property of the hUGDH hexamer (Figures 1B and 2B). Thus, we believe that hUGDH hysteresis is due to the hexamer undergoing a transition from a less active to a more active state (compare k_{obs} values in panels C and G of Figure 2). However, it is also possible that the slow isomerization occurs in the $hUGDH_{K94E}$ dimer but is not observed because the turnover rate is ∼48 times slower than that of the wild-type enzyme.

Evidence for Cofactor-Induced Asymmetry in the hUGDH Hexamer. Steady-state analysis shows that NAD^+ induces negative cooperativity in hUGDH (Figure 3A). Negative cooperativity in an oligomeric complex occurs when substrate binding weakens the affinity of active sites in adjacent subunits.[29] However, an apparent cooperativity can be observed in the steady-state analysis of hysteretic enzymes due to an underlying kinetic mechanism.[30] Kinetic cooperativity can be distinguished from "true" substrate-induced cooperativity using equilibrium binding studies.[6,10] Our binding studies show that the formation of the hUGDH:UDG:NADH complex displays strong NADH-dependent negative cooperativity (Figure 4C). Because the substrate saturation curves of the $hUGDH_{K94E}$ dimer are hyperbolic, the negative cooperativity appears to be a property of the hexamer (Figure 3C,D).

Negative cooperativity can also be interpreted as an asymmetry induced by substrate binding.[31] The absence of cooperativity in the hUGDH:NADH complex is good evidence that the asymmetry is a property of the ternary complex (Figure 4B). However, the difference in the Hill coefficients for binding of NAD^+ (0.74 ± 0.03) and NADH (0.42 ± 0.05) to the hUGDH:UDG complex suggests that there may be significant structural differences between the active and abortive ternary complexes (Figures 3A and 4C and Table 1). It is possible that the difference in the Hill coefficients is due to a small amount of product inhibition. We have shown that NADH inhibition oblates negative cooperativity (Figure 6). We interpret this to mean that the intersubunit communication required for cooperativity is disrupted in a mixed NAD/NADH ternary complex. While the enzyme concentration used in the steady-state analysis (230 nM) was chosen to minimize product inhibition, it may still have produced enough NADH to weaken the intersubunit communication and reduce the degree of cooperativity observed in steady-state analysis.

A Structure-Based Hypothesis for the Substrate-Induced Isomerization and Negative Cooperativity in hUGDH. It is tempting to speculate that the slow enzyme isomerization produces the asymmetric complex that is responsible for the negative cooperativity in hUGDH. To investigate this hypothesis, we studied the transient processes associated with the stepwise formation of the hUGDH:UDG:-NADH complex (Figure 7A). First, we examined the formation of the hUGDH:UDG and hUGDH:NADH binary complexes. The fluorescence signal for binding of UDG to hUGDH is too fast and too weak to accurately measure, but it is followed by

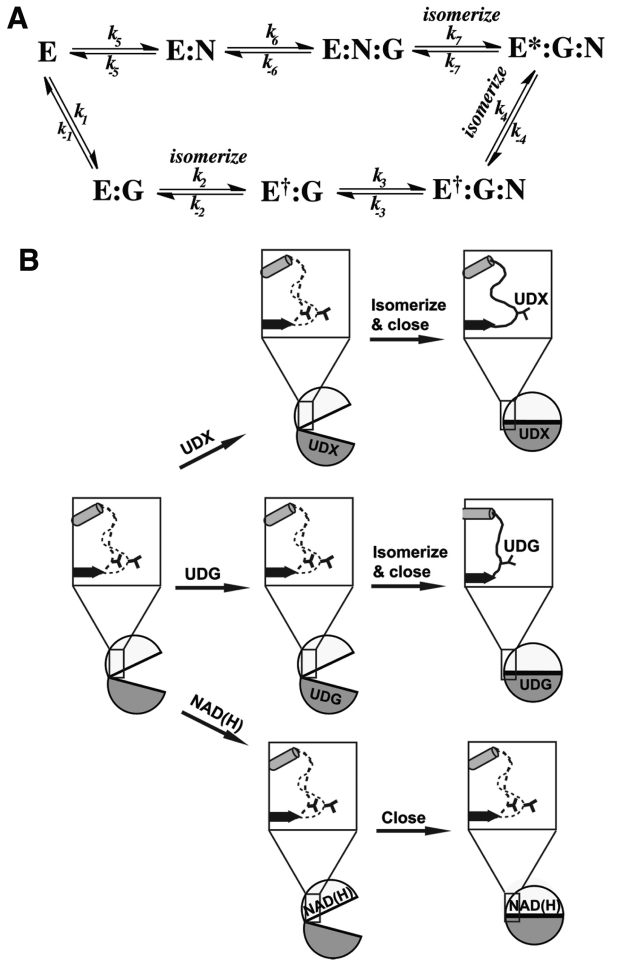

Figure 7. Enzyme isomerizations in the stepwise formation of the abortive ternary complex, hUGDH:UDG:NADH. (A) Scheme showing the stepwise binding of ligands UDG (G) and NADH (N) to hUGDH (E) to form the E*:G:N complex. Individual rate constants derived from stopped-flow kinetics are discussed in the text and listed in Table 2. The three isomerization steps are labeled. (B) Cartoon model of a hUGDH monomer showing the relationship between domain rotation and the allosteric response of hUGDH. Substrate and cofactor binding domains are depicted as gray and white semicircles, respectively. The Thr131-loop/α6 allosteric switch is depicted as an ensemble of conformational states (dashed lines) connecting the α6 helix (gray cylinder) to a β strand (black arrow). Substrate (UDG) or inhibitor (UDX) can bind to hUGDH, but domain closure can occur only if the Thr131-loop/α6 switch isomerizes to the appropriate state (solid line). The cofactor [NAD(H)] can bind, and domains close with the switch in either state.

dx.doi.org/10.1021/bi301593c | Biochemistry 2013, 52, 1456−1465

what appears to be a slower ligand-induced isomerization to form a binary hUGDH†:UDG complex (Figures 5A and 7A). In contrast, binding of NADH to hUGDH is a slow process consistent with the second-order formation of the hUGDH:NADH complex (Figure 5D). It is possible that the two distinct processes associated with substrate and cofactor addition are related to the unusual feedback inhibition mechanism of hUGDH.[15,16,18] Briefly, the domains of hUGDH rotate open to allow either UDG or the feedback inhibitor UDP-xylose (UDX) to bind to the active site (Figure 7B).[15,17] With the domains open, the Thr131-loop/α6 helix (the allosteric switch) can adopt either the active or the inactive conformation.[15,18] UDG can bind with the Thr131-loop/α6 helix in either conformation; however, the domains can close only if the allosteric switch selects the active conformation. We believe that the UDG-induced isomerization may be due to the allosteric switch converging to the active conformation (Figure 7B). This interpretation predicts that UDX binding will also induce a lag as the allosteric switch slowly adopts the inactive conformation (Figure 7B). In fact, Gainey and Phelps have reported that binding of UDX to UGDH also displays hysteresis.[32] The absence of an isomerization in the formation of the hUGDH:NADH complex is also consistent with this hypothesis (Figure 5D). Our previous structural work has shown that hUGDH domains can close to bind NADH with the allosteric switch in either conformation (Figure 7B).[15,18]

Next, we examined the transient processes associated with the formation of the hUGDH*:UDG:NADH complex (Figure 7A). Binding of UDG to the hUGDH:NADH complex is detected as a single process consistent with a ligand-induced isomerization (Figure 5E). We assume the initial UDG binding event is too fast or the florescence signal is too small to be detected, similar to what we observed for the binding of UDG to hUGDH alone (Figure 5A). It is likely that the isomerization prior to the formation of the ternary complex is associated with the asymmetry responsible for the negative cooperativity. This hypothesis is supported by the equilibrium studies that reveal negative cooperativity in the ternary complex, not the binary (Figure 4B,C).

The abortive ternary complex can also be formed by binding of NADH to the hUGDH†:UDG complex. The stopped-flow data reveal two phases associated with NADH binding, a fast association event followed by a slower isomerization (Figure 5B,C). The fact that the equilibrium constant for the isomerization (K_3) is ~10-fold higher than the dissociation constant for NADH binding (k_{-3}/k_3) indicates the presence of at least one additional transient process prior to the isomerization that is not observed in the fluorescence decay (Figure 7A and Table 2). We note that the dissociation constant k_{-3}/k_3 (8.1 μM) is close to the K_d (4.2 μM) for the abortive ternary complex that we determined in equilibrium binding studies (Tables 1 and 2). It would appear that the hUGDH†:UDG complex has high-affinity NADH binding sites, and the formation of the ternary complex produces the lower-affinity sites responsible for negative cooperativity.

We are not the first to propose asymmetry in the hUGDH ternary complex. Half-of-the-sites activity, in which only three of the active sites turn over product, has been reported for UGDH.[33−35] Half-of-the-sites activity is an extreme form of negative cooperativity with an obligatory structural asymmetry.[36] Because of this constraint, the steady-state kinetics of an enzyme with half-of-the-sites activity will be hyperbolic. On the other hand, in an enzyme displaying negative cooperativity, the low-affinity sites can still be occupied and turnover, resulting in nonhyperbolic kinetics. Our steady-state and equilibrium studies clearly show negative cooperativity in the ternary complex of hUGDH (Figures 3A and 4C). It may be that the earlier reports misidentified half-of-the-sites activity or that the physiologically relevant pH in our assays has altered the mechanism.

Our equilibrium binding data and steady-state analysis show that the hUGDH:UDG:NADH complex displays negative cooperativity in solution (Figure 4C). However, the hUGDH:UDG:NADH crystal structure is a hexamer with no obvious asymmetry.[17] It may be that the vast excess of cofactor (5 mM) used during crystallization saturated the low-affinity sites to produce the symmetrical complex. On the other hand, the structure of the alternate abortive ternary complex, hUGDH:UGA:NAD+ reveals a compelling asymmetry; the "top" three molecules adopt an open domain conformation, and the "bottom" three are closed.[16]

Physiological Relevance of hUGDH Hysteresis. Hysteresis can play an essential role in regulating enzyme activity.[5] For example, hysteresis in human pancreatic glucokinase regulates insulin secretion by slowing the response of the enzyme to temporary spikes in blood glucose levels.[7−9] Thus, insulin is secreted only in the presence of sustained high levels of glucose. In the case of hUGDH, the substrate UDG is an important metabolite in several biochemical pathways. For example, the conversion of D-galactose to UDG in the Leloir pathway can result in a sharp increase in UDG flux. Hysteresis will prevent hUGDH from competing with other important metabolic pathways (like glycolysis) when there are sudden increases in the flux of UDG.

AUTHOR INFORMATION

Corresponding Author

*Phone: (706) 583-0304. Fax: (706) 542-1738. E-mail: zac@bmb.uga.edu.

Funding

Funding from the American Cancer Society (Grant RSG0918401DMC) and the University of Georgia Research Alliance to Z.A.W. is gratefully acknowledged.

Notes

The authors declare no competing financial interest.

ABBREVIATIONS

hUGDH, human UDP-α-D-glucose 6-dehydrogenase; UDP, uridine diphosphate; UGA, UDP-α-D-glucuronic acid; UDX, UDP-α-D-xylose.

REFERENCES

(1) Strominger, J. L., Kalckar, H. M., Axelrod, J., and Maxwell, E. S. (1954) Enzymatic Oxidation of Uridine Diphosphate Glucose to Uridine Diphsphate Glucuronic Acid. *J. Am. Chem. Soc. 76*, 6411−6412.

(2) Ordman, A. B., and Kirkwood, S. (1977) UDPglucose dehydrogenase. Kinetics and their mechanistic implications. *Biochim. Biophys. Acta 481*, 25−32.

(3) Campbell, R. E., Sala, R. F., van de Rijn, I., and Tanner, M. E. (1997) Properties and kinetic analysis of UDP-glucose dehydrogenase from group A streptococci. Irreversible inhibition by UDP-chloroacetol. *J. Biol. Chem. 272*, 3416−3422.

(4) Dickinson, F. M. (1988) Studies on the unusual behaviour of bovine liver UDP-glucose dehydrogenase in assays at acid and neutral

pH and on the presence of tightly bound nucleotide material in purified preparations of this enzyme. *Biochem. J. 255*, 775−780.
(5) Frieden, C. (1970) Kinetic aspects of regulation of metabolic processes. The hysteretic enzyme concept. *J. Biol. Chem. 245*, 5788−5799.
(6) Neet, K. E., and Ainslie, G. R., Jr. (1980) Hysteretic enzymes. *Methods Enzymol. 64*, 192−226.
(7) Neet, K. E., Keenan, R. P., and Tippett, P. S. (1990) Observation of a kinetic slow transition in monomeric glucokinase. *Biochemistry 29*, 770−777.
(8) Heredia, V. V., Thomson, J., Nettleton, D., and Sun, S. (2006) Glucose-induced conformational changes in glucokinase mediate allosteric regulation: Transient kinetic analysis. *Biochemistry 45*, 7553−7562.
(9) Kim, Y. B., Kalinowski, S. S., and Marcinkeviciene, J. (2007) A pre-steady state analysis of ligand binding to human glucokinase: Evidence for a preexisting equilibrium. *Biochemistry 46*, 1423−1431.
(10) Ainslie, G. R., Jr., Shill, J. P., and Neet, K. E. (1972) Transients and cooperativity. A slow transition model for relating transients and cooperative kinetics of enzymes. *J. Biol. Chem. 247*, 7088−7096.
(11) Kurganov, B. I., Dorozhko, A. I., Kagan, Z. S., and Yakovlev, V. A. (1976) The theoretical analysis of kinetic behaviour of "hysteretic" allosteric enzymes. II. The dissociating and associating enzymic systems in which the rate of installation of equilibrium between the oligomeric forms is small in comparison with that of enzymatic reaction. *J. Theor. Biol. 60*, 271−286.
(12) Kurganov, B. I., Dorozhko, A. K., Kagan, Z. S., and Yakovlev, V. A. (1976) The theoretical analysis of kinetic behaviour of kinetic behaviour of "hysteretic" allosteric enzymes. III. Dissociating and associating enzyme systems in which the rate of installation of equilibrium between the oligomeric forms in comparable to that of enzymatic reaction. *J. Theor. Biol. 60*, 287−299.
(13) Ricard, J., Buc, J., and Meunier, J. C. (1977) Enzyme memory. 1. A transient kinetic study of wheat-germ hexokinase LI. *Eur. J. Biochem. 80*, 581−592.
(14) Buc, J., Ricard, J., and Meunier, J. C. (1977) Enzyme memory. 2. Kinetics and thermodynamics of the slow conformation changes of wheat-germ hexokinase LI. *Eur. J. Biochem. 80*, 593−601.
(15) Sennett, N. C., Kadirvelraj, R., and Wood, Z. A. (2011) Conformational flexibility in the allosteric regulation of human UDP-α-D-glucose 6-dehydrogenase. *Biochemistry 50*, 9651−9663.
(16) Sennett, N. C., Kadirvelraj, R., and Wood, Z. A. (2012) Cofactor binding triggers a molecular switch to allosterically activate human UDP-α-D-glucose 6-dehydrogenase. *Biochemistry 51*, 9364−9374.
(17) Egger, S., Chaikuad, A., Kavanagh, K. L., Oppermann, U., and Nidetzky, B. (2011) Structure and mechanism of human UDP-glucose 6-dehydrogenase. *J. Biol. Chem. 286*, 23877−23887.
(18) Kadirvelraj, R., Sennett, N. C., Polizzi, S. J., Weitzel, S., and Wood, Z. A. (2011) Role of packing defects in the evolution of allostery and induced fit in human UDP-glucose dehydrogenase. *Biochemistry 50*, 5780−5789.
(19) Copeland, R. A. (2000) *Enzymes: A practical introduction to structure, mechanism and data analysis*, 2nd ed., Wiley-VCH, New York.
(20) Cornish-Bowden, A. (2001) Detection of errors of interpretation in experiments in enzyme kinetics. *Methods 24*, 181−190.
(21) Lakowicz, J. R. (2006) *Principles of Fluorescence Spectroscopy*, 3rd ed., Springer, Berlin.
(22) Palmier, M. O., and Van Doren, S. R. (2007) Rapid determination of enzyme kinetics from fluorescence: Overcoming the inner filter effect. *Anal. Biochem. 371*, 43−51.
(23) Bernasconi, C. F. (1976) *Relaxation Kinetics*, Academic Press, San Diego.
(24) Frieden, C. (1979) Slow transitions and hysteretic behavior in enzymes. *Annu. Rev. Biochem. 48*, 471−489.
(25) Bates, D. J., and Frieden, C. (1973) Treatment of enzyme kinetic data. 3. The use of the full time course of a reaction, as examined by computer simulation, in defining enzyme mechanisms. *J. Biol. Chem. 248*, 7878−7884.
(26) Bates, D. J., and Frieden, C. (1973) Full time course studies on the oxidation of reduced coenzyme by bovine liver glutamate dehydrogenase. Use of computer simulation to obtain rate and dissociation constants. *J. Biol. Chem. 248*, 7885−7890.
(27) Zalitis, J., and Feingold, D. S. (1968) The mechanism of action of UDPG dehydrogenase. *Biochem. Biophys. Res. Commun. 31*, 693−698.
(28) Molz, R. J., and Danishefsky, I. (1971) Uridine diphosphate glucose dehydrogenase of rat tissue. *Biochim. Biophys. Acta 250*, 6−13.
(29) Levitzki, A., and Koshland, D. E., Jr. (1969) Negative cooperativity in regulatory enzymes. *Proc. Natl. Acad. Sci. U.S.A. 62*, 1121−1128.
(30) Frieden, C., and Nichol, L. W., Eds. (1981) *Protein-Protein Interactions*, Wiley, New York.
(31) Koshland, D. E., Jr. (1996) The structural basis of negative cooperativity: Receptors and enzymes. *Curr. Opin. Struct. Biol. 6*, 757−761.
(32) Gainey, P. A., and Phelps, C. F. (1975) Interactions of urdine diphosphate glucose dehydrogenase with the inhibitor urdine diphosphate xylose. *Biochem. J. 145*, 129−134.
(33) Franzen, J. S., Kuo, I., Eichler, A. J., and Feingold, D. S. (1973) UDP-glucose dehydrogenase: Substrate binding stoichiometry and affinity. *Biochem. Biophys. Res. Commun. 50*, 517−523.
(34) Gainey, P. A., and Phelps, C. F. (1974) The binding of oxidized and reduced nicotinamide-adenine dinucleotides to bovine liver uridine diphosphate glucose dehydrogenase. *Biochem. J. 141*, 667−673.
(35) Franzen, J. S., Marchetti, P., Ishman, R., and Ashcom, J. (1978) Half-sites oxidation of bovine liver uridine diphosphate glucose dehydrogenase. *Biochem. J. 173*, 701−704.
(36) Levitzki, A., Stallcup, W. B., and Koshland, D. E., Jr. (1971) Half-of-the-sites reactivity and the conformational states of cytidine triphosphate synthetase. *Biochemistry 10*, 3371−3378.
(37) Segel, I. H. (1993) *Enzyme Kinetics*, Wiley, New York.